- Technical Paper -

THE EFFECT OF SEAWATER MIXING ON CORROSION OF STEEL BAR IN 36-YEARS OLD RC BEAMS UNDER MARINE TIDAL ENVIRONMENT

Dahlia Patah[*1], Hidenori HAMADA[*2], Yasutaka SAGAWA[*3] and Daisuke YAMAMOTO[*4]

ABSTRACT

Visual observation, chloride ingress, porosity, and corrosion of steel bars in RC beam made with seawater and tap water were investigated in this paper based on 36 years of exposure under marine tidal environment. After long-term exposure, seawater mixing shows better performance against corrosion of steel bar as well as strength, concrete resistance, oxygen permeability and microstructure compared with tap water mixing. It shows high possibility to use seawater as mixing water with precautions, such as minimum 50mm in cover depth which has influence significantly for the service life of RC structure.

Keywords: seawater mixing, corrosion, corroded area, microstructure, RC beam

1. INTRODUCTION

In the concrete industry, several billion tons of fresh water are used annually in the mixing, curing, and cleaning around the world. In the viewpoint of saving fresh water, the possibilities of using seawater-mixed concrete should be investigated comprehensively. Further, if the use of seawater as mixing water in concrete is reliable, it would be very convenient and economical in construction, especially in coastal works and isolated island. JSCE committee reported seawater as mixing water should be avoided to be used in RC structures because of the risk of early corrosion of reinforcement induced by chloride in seawater compounds. However, in the case of unavoidable situation, seawater as mixing water is recommended only for plain concrete [1]. Furthermore, Mohammed et al. reported that seawater mixing caused an earlier gain in the strength and improved the microstructure of concrete compared to tap water mixing. In addition, the deterioration in concrete strength was not encountered due to the acceleration of hydration process in the presence of chlorides in the used seawater after 15-years of exposure in a tidal pool [2]. Fukute and Hamada reported seawater-mixed concrete did not affect to corroded area very much after 20 years of exposure [3].

This study aims: (1) to evaluate the effect of seawater mixing on deterioration and steel corrosion of RC beam under service load after 36-years of exposure; (2) to understand how far the contribution of seawater mixing and concrete cover on durability of RC structure after long-term exposure particularly in marine environment. Visual observation, chloride ingress, microstructure, and corrosion of steel bars in RC beams (electrochemical and physical) were evaluated and summarized in this paper.

2. TEST PROGRAMS

2.1 Materials

The investigations of four RC beam specimens were carried out. The RC beam specimens were mixed with tap water and seawater. The cement type was Ordinary Portland Cement (OPC). The detailed information of mix proportions of concrete is unavailable. Water-cement ratios (W/C) were 55% and 65%. The density of concrete was 2,398kg/m^3. Two groups of the RC beam were noted “Group I” as W/C of 55% with introduced stress of bar 300MPa (Bending moment M=7.97kNm) and “Group II” as W/C of 65% with stress load of bar 100MPa (Bending moment M=2.66kNm). Summary of RC beam is shown in Table 1.

Table 1 Summary of RC beam

Group	Specimen	W/C (%)	M (kNm)	Mixing water
I	55-L3-TW	55	7.97	Tap water
	55-L3-SW	55	7.97	Seawater
II	65-L1-TW	65	2.66	Tap water
	65-L1-SW	65	2.66	Seawater

The layout details of the RC beam were shown in Fig. 1. Dimensions of beam were 120x150x1200 mm. Three deformed steel bars of diameter 10mm were embedded at 20, 30, and 50mm of cover depth from the two sides in the beam. The four sides of the RC beam were noted “Side C” as compression side, “Side T” as tension side, “Side F” and “Side B as front and back side respectively.

The investigations were carried out after 36-years of exposure. The RC beams were cast and then stored in a tidal pool under constant bending load at the Port and

*1 Graduate School of Engineering, Kyushu University, M. Eng., JCI Student Member
*2 Professor, Dept. of Civil and Structural Engineering, Kyushu University, Dr. Eng., JCI Fellow Member
*3 Associate Prof., Dept. of Civil and Structural Engineering, Kyushu University, Dr. Eng., JCI Member
*4 Technical Officer, Dept. of Civil and Structural Engineering, Kyushu University, Dr. Eng., JCI Member

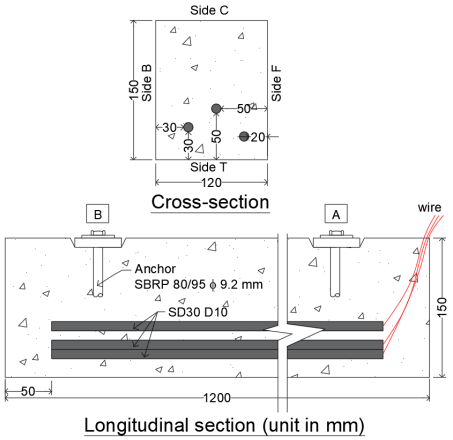

Fig 1 Layout details of the RC beam

Airport Research Institute (PARI) laboratory in Yokosuka-Japan for 32 years. Then they were moved to exposure site at Kyushu University followed by four years' exposure under outside natural environment, without bending load.

2.2 Experimental methods

(1) Visual observation of crack

For each side, crack map was drawn, focusing on locations of longitudinal and transversal cracks due to corrosion and service load, respectively. On these maps, lengths, widths, and depths of each referred crack are also indicated.

(2) Electrochemical analysis

For electrochemical evaluation of steel bars, half-cell potential (HCP), anodic polarization curve (APC), and oxygen permeability were measured in cover depths of 20, 30 and 50mm. The HCP was measured by using the silver/silver chloride reference electrode (Ag/AgCl) after 30-min pre-wetting of beam surface. Then, the potential value was converted to the value against copper/copper sulfate reference electrode (CSE). The threshold limit of HCP is assumed to be -350mV as per ASTM C 876-15 [4].

For APC, the potential of the steel bar was swept to +700mV from rest potential with a sweep rate of 50mV/min by a potentiostat, and the current was recorded continuously. The maximum current obtained from APC was a parameter to judge "grade of passivity" based on the methodology proposed by Otsuki. [5].

The constant current density (i_{lim}) over the steel bars at cover depth of 20, 30 and 50mm was measured. The i_{lim} was measured by using a potentiostat. The potential of the steel bar was set to -1V and held constant then the current was recorded continuously. When measurements began, current was a maximum then gradually falling until reaching an almost constant value after kept in 24-hours. The rate of oxygen permeability was obtained from the i_{lim} using the following Eq. (1)

$$dQ / dt = - i_{lim} / (n \, . \, F) \quad (1)$$

where,

dQ/dt : oxygen permeability in mol/cm^2/s

i_{lim} : constant current density in A/cm^2

n : number of electrons (4)

F : Faradays constant (96,500 coulombs/mol)

(3) Carbonation and chloride analysis

The carbonation depth of the RC beam was evaluated after spraying 1% phenolphthalein solution on freshly cut or broken surfaces. Total and water-soluble chloride concentration were measured at certain depths of specimens. To measure chloride concentration, cylinder specimen was taken by coring method. Then, specimens were cut in five layers from the surface of concrete through the depth with 10mm thick for each layer and crushed into powder. The samples were powdered by a vibrating mill. Total chloride and water-soluble chloride concentration were measured as per JIS A1154 and JCI-SC4, respectively.

(4) Quality of concrete

For quality of concrete, compressive strength, electrical resistivity and porosity were measured. The compressive strength of concrete was measured as per JIS A1108. Cylinder specimens in size of ϕ50x100mm were taken by coring method. The average of five cylinder specimens was determined for each beam.

The electrical resistivity was measured by using Wenner probe. The resistivity of concrete from the average of three times measurement was determined.

The porosity of concrete was measured at depths of 60mm from the surface. Mortar pieces were cut into five mm-thick cube slice samples. The sample was immersed in acetone for 15-min to stop the hydration of cement and then dried in the vacuum desiccator for two days. Then the porosity of concrete was evaluated by mercury intrusion porosimeter (MIP) with pressure of 33,000psi (227MPa), and the surface tension and contact angle of mercury were 485dynes/cm and 130°, respectively.

(5) Physical analysis

For physical evaluation of corrosion, the corroded area of the steel bars embedded at different cover depths was measured. Corroded area of steel bar was measured after completely removed from the RC beam specimen. The corroded area over the steel bars was traced over a transparent paper and then corroded area of steel bar was calculated using software ImageJ v1.49.

3. RESULT AND DISCUSSION

3.1 Crack map

Visual observation enables to describe a global overview of the damage state of the RC beam after long-term exposure. Some transversal and longitudinal cracks due to corrosion attack beside bending load can be mainly observed on the beams for both group (Fig. 2). It was observed that tap water mixing appears much more rough surface due to environmental condition and some spots of rust stains appear at area of corrosion-induced cracks compared to seawater mixing (both group). Visibly, cracks induced corrosion occurred longitudinal along the steel bar and parallel to steel bar on the end part (point A and B) of beam. As well as transverse cracks from introduced bending moment were generated from tension side of the beam. Cracking had generalized along the tensile area and cracks appeared in the end part of the beams. On the contrary, compressive area showed no crack. For Group I, the maximum crack width of

seawater mixing (1.2mm) was larger than tap water mixing (0.5mm). However, for Group II, the maximum crack width of seawater was same with tap water mixing (1.5mm). In addition, the crack depth value already through the concrete cover for both group.

3.2 Electrochemical analysis

The HCP of the steel bars embedded at different cover depths are shown in Fig. 3. From these figures, negative potentials were observed for tap water mixing both group in all cases concrete cover, and the potential value was less than -350mV and categorized 90% corrosion. The tendencies observed in cover depth 20mm are that the potential values of seawater mixing (both group) showed very negative value than tap water mixing and categorized 90% corrosion. In contrary, at

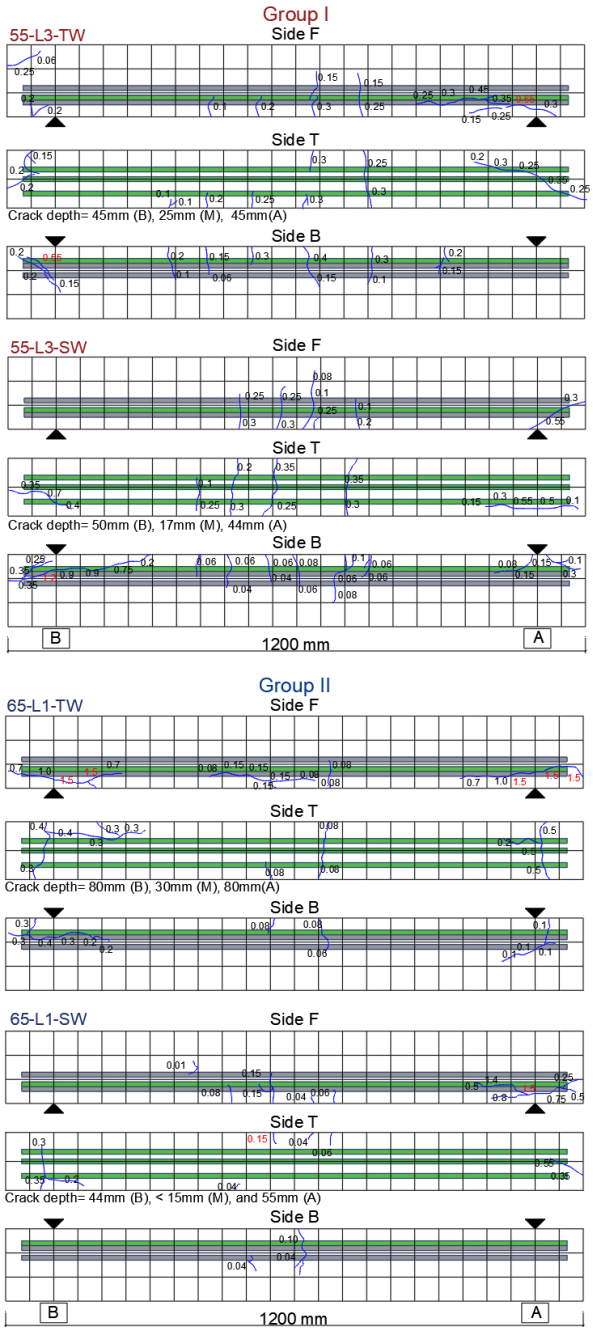

Fig. 2 Crack map (Group I and II)

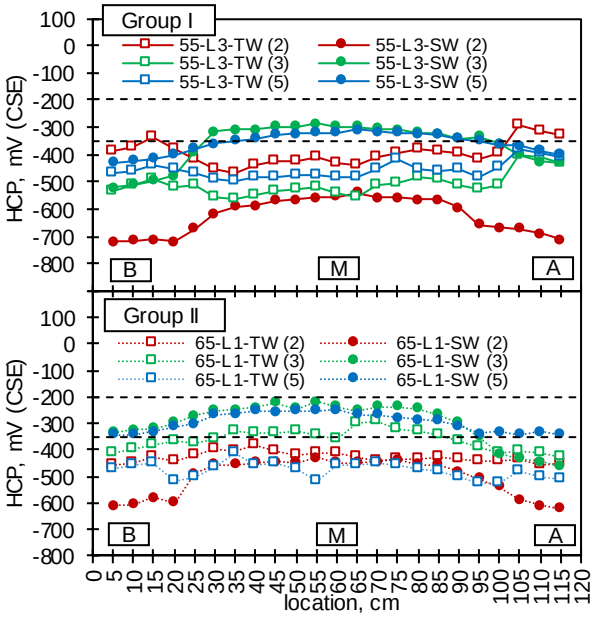

Fig. 3 Half-cell potential (Group I and II)

cover depth 30 and 50mm, the potential of seawater mixing (both group) became a positive value and categorized uncertainly in the middle part (Point M), however, in end part (Point A and B) the potential became negative value and categorized 90% corrosion. The possible reason may be due to the number, width, and depth of crack at the end part of beam. Importantly, concrete cover with 20mm influences on the HCP value much more than mixing water. However, concrete cover 30 and 50mm showed the HCP value for seawater superior to tap water mixing. Implies that after concrete cover with 30 and 50mm, mixing water influences much more than concrete cover on HCP value.

The APC of the steel bars embedded at different cover depths is shown in Fig. 4. From these figures, tap water mixing of both group shows higher current density and indicated higher corrosion activity of the steel bars. In contrast, the ACP of seawater mixing of both group shows lower current density. The passivity grades of tap

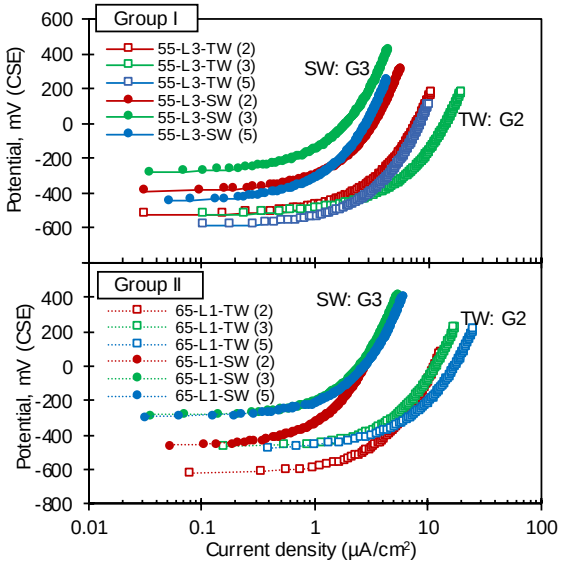

Fig. 4 Anodic polarization curve (Group I and II)

water and seawater mixing were categorized in Grade 2 and Grade 3, respectively, for all concrete cover (both group). The seawater mixing shows better passivity compared to tap water mixing. A better grade of passivity for the steel bars embedded in seawater indicates less corrosion activity, and this corresponds to HCP value. Corrosion activity broke the passivity film of the steel bar and released much more electron. This mechanism leads to a very negative value of HCP value.

Oxygen permeability at different cover depths is estimated from the measured i_{lim}. The results are shown in Fig. 5. From this figure, it was clearly seen that the oxygen permeability became low as increasing cover depth. In addition, oxygen permeability was lower in seawater mixing than tap water mixing in all cover depth (both group). These results support that seawater mixing is effective for controlling the oxygen permeability through the concrete cover, therefore, retarding both anodic and cathodic reactions of steel bars in concrete.

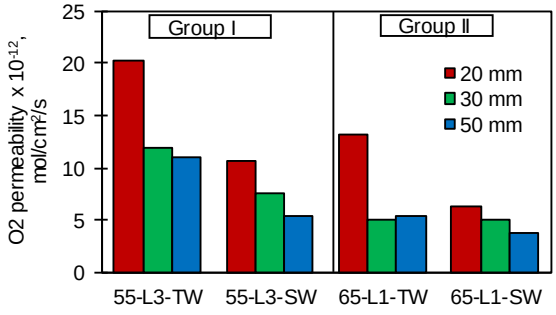

Fig. 5 Oxygen permeability

3.3 Carbonation depth and chloride ingress

The carbonation depth was almost negligible for seawater and tap water mixing (both group). Only in a few spots, maximum depth is 1-1.5mm, and it was limited to surface only. Thus, the steel bars in concrete located at 20, 30, and 50mm of cover depths were free from carbonation-induced corrosion, and corrosion of steel bar must be induced by chloride ingress.

Total chloride, water-soluble chloride and bond chloride in concrete are summarized in Table 2. Chloride ingress pattern for tap water and seawater mixing from surface to half part was same, which indicate that chloride induces already saturated after long-term exposure. At the steel bars depth, the measured values of water-soluble chloride (more than 7kg/m^3 for both group) exceed the threshold limit of 1.2kg/m^3 generally pointed out in JSCE. It is generally assumed that for higher chloride content the corrosion can be initiated at the steel bar surface. These results explain that active corrosion due to chloride ingress can take place at steel bar surface. Also, this is probably due to mechanical damage of the tensile area due to bending load which leads to a significant increase in the chloride diffusion coefficient. In addition, for Group I, the amount of water-soluble chloride for seawater mixing was lower than tap water mixing. However, for Group II, the amount of water-soluble chloride of seawater mixing was higher than tap water probably due to the initial chloride from the seawater. In addition, the bound chloride was higher for seawater mixing compared with tap water mixing for both group (it is almost 2kg/m^3 at cover depth 35 and 55mm). Ismail et al. reported that after the chloride ingress, some chlorides could be attached to the pore walls or cement products and react with them, which is called chloride binding [6]. The chloride binding is commonly classified as the physical binding and chemical binding. Physical binding occurs when chloride ions transport through the C-S-H type gel surface, and occurs due to electrostatic or Van der Waals forces between chloride and the gel [6]. Chemical binding can be defined as chloride ions interact with C-S-H gel by several mechanisms such as chemisorption into the C-S-H layers, in C-S-H spaces, or becoming bound in the lattice or ion exchange sites of C-S-H gel. These bound chloride ions can give rise to an altered matrix microstructure. The chemically bound chlorides in the cementitious materials at the beginning react with the main OPC component, C_3A [7].

Table 2 Chloride concentration

Group	Specimen	Cover depth (mm)	Total chloride (kg/m^3)	Water-soluble chloride (kg/m^3)	Bound chloride (kg/m^3)
I	55-L3-TW	20	12.67	12.15	0.52
		30	13.10	12.06	1.04
		50	12.40	11.23	1.16
	55-L3-SW	20	8.42	8.35	0.06
		30	10.01	7.92	2.09
		50	9.00	7.07	1.93
II	65-L1-TW	20	8.06	7.19	0.87
		30	9.02	7.60	1.42
		50	9.65	8.24	1.41
	65-L1-SW	20	10.31	9.88	0.43
		30	10.70	8.65	2.05
		50	11.32	9.20	2.12

3.4 Quality of concrete

Compressive strength, electrical resistance and total pore volume of concrete are summarized in Table 3. After 36-years of exposure, seawater mixing showed higher strength, denser and higher electrical resistance than tap water mixing (both group). Interestingly, the strength of seawater mixing showed 10MPa larger than tap water mixing. The seawater/tap water strength ratio was 1.2 at long-term exposure (both group). This tendency was also reported by Fukute and Hamada [3] and Adiwijaya [8].

Table 3 Summary of quality of concrete

Group	Type	Compressive strength (MPa)	Total pore volume (cm^3/g)	Electrical resistance (kΩcm)
I	55-L3-TW	49.36	0.038	17.39
	55-L3-SW	59.10	0.036	35.22
II	65-L1-TW	50.21	0.059	21.60
	65-L1-SW	60.09	0.039	27.90

Mean cumulative pore volume and incremental pore volume of concrete mixed with tap water and seawater are shown in Fig.7 and Fig. 8, respectively. Interestingly, it is found that pore distribution of seawater mixing is denser and finer compared than tap

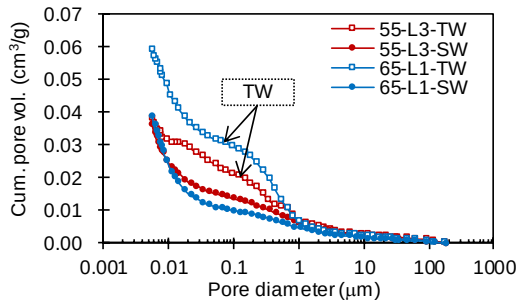

Fig. 7 Cumulative pore volume

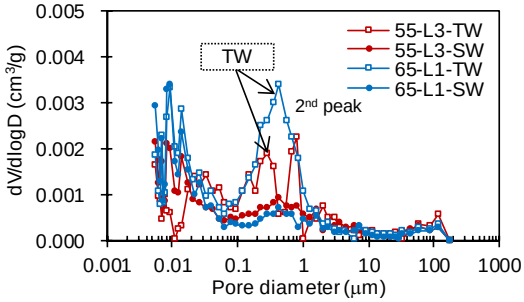

Fig. 8 Incremental pore volume

water mixing in both group. In addition, tap water mixing has second peak in incremental pore volume, and for seawater mixing it is almost smooth. These results are due to higher concrete resistance, higher strength, and chloride in seawater compounds. Midgley et al. reported that for seawater mixing, the transformation of the hydration phase from CAH_{10} to C_3AH_6 had not occurred. By using the NaCl solution as the Cl^- source to study the pore size distribution of cement paste under chloride ingress, it was found that the intrusion of chloride ion leads to more fine pores and less big pores. As soon as the reaction begins, the binding between the chloride ion and cement product can modify the shape of concrete microstructure [9]. Higher concrete resistance of seawater mixing leads to the high resistivity against chloride-induced corrosion. Considerable delay of corrosion reaction which leads the increase of steel bar volume. Inner pressure as the result of increment steel bar volume is notable on crack appearance. This corrosion activity correlated in Fig. 2 which shows seawater mixing has small number of cracks.

3.5 Corroded area

The appearance of corroded area and distribution of corroded areas described in percent degree on the steel bars at different cover depths are shown in Fig. 9 and Fig.10, respectively. From the figure it can be observed the rust was spotted and generated along the steel bar in all cases of cover depth of 55-L3-TW. However, for 65-L1-TW and 55-L3-SW only in cover depth of 20mm. On the contrary, the rust was concentrated and dense only in the end part of beam in all cases of cover depth for 65-L1-SW. While 65-L1-TW and 55-L3-SW discovered only in cover depth 30 and 50mm. These results correspond to the HCP data explained previously. The reason for the more corrosion at the end part may be due to chloride ingress from the end part of beam, therefore, the most damaged zones were close to the position at the maximum cracks width and depth.

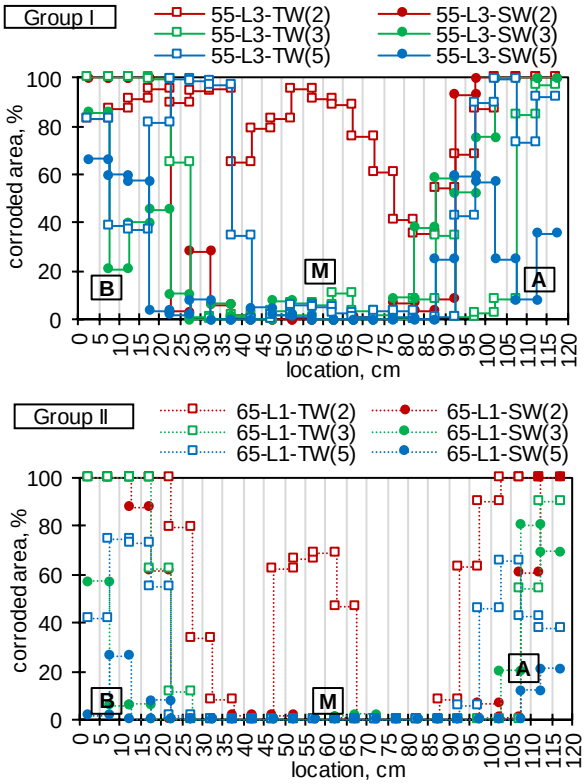

Fig. 10 Corroded area (Group I and II)

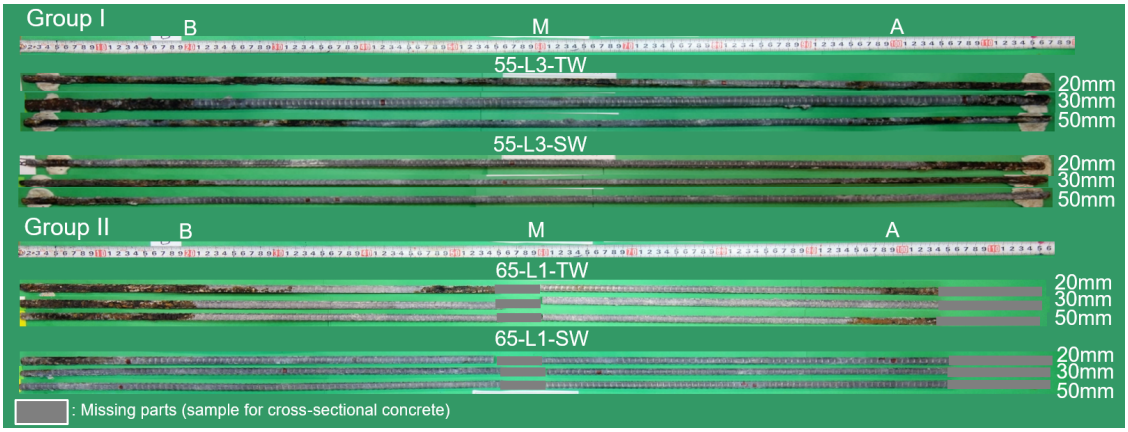

Fig. 9 The appearance of corroded area

The results of the total corroded area of steel bar are summarized in Table 4. The smaller corroded area is found in most of deeper cover depths. Interestingly, it can be noted that the total corroded area for seawater mixing in all cases of cover depth is almost half of tap water mixing (both group), except for the cover depth 30mm of Group I, which is almost same total corroded area value. From this, it can be estimated that seawater mixing had better degree of passivity as discussed previously in electrical measurements. The result leads to understanding that seawater mixing has high resistivity against chloride-induced corrosion. The result shows strong correlation on crack appearance in Fig.2 and supported by actual corroded area that seawater mixing has lower corrosion activity. The possible reason why seawater mixing showed smaller corroded area than tap water mixing is that the corrosion rate for seawater mixing was controlled due to the lower chloride ingress as well as lower oxygen permeability, and also higher concrete resistance.

Table 4 Corroded area of steel bars

Cover depth (mm)	Total corroded area (%)			
	Group I		Group II	
	55-L3-TW	55-L3-SW	65-L1-TW	65-L1-SW
20	81.46	42.40	53.06	24.01
30	32.84	33.93	20.04	11.46
50	44.04	18.00	19.69	3.47

The result demonstrated that seawater mixing showed better resistant performance against the corrosion of steel bar. Actually, seawater mixing generated 20% of total corroded area, however, passivity grade was more reasonable than tap water mixing. For the sea water mixing in Group I (W/C= 55% and M=7.97kNm), the amount of corroded area was less than 20% with concrete cover 50mm. Therefore, seawater mixing may be more reasonable for application in a case such as marine exposure condition. It is also interesting result on seawater mixing in Group II (W/C =65% and M=2.66kNm), that is, the amount of corroded area was only 3.47%. And, the smaller bending moment (Group II) reduced the corroded area. Therefore, the maximum bending moment should be taken into the acount. It is also considered that concrete cover is one key factor for reasonable use of seawater as mixing water.

4. CONCLUSIONS

Based on the results of this study, it was demonstrated that the use of seawater as mixing water helps to maintain the robust performance throughout a long exposure period of 36-years. The following conclusions can be drawn from this experimental study:

(1) The use of seawater as mixing water improved concrete strength, concrete resistance, oxygen permeability resistance and maintained very dense microstructure, in RC beam after 36-years of marine exposure.

(2) The dense microstructure of seawater mixed concrete maintained a high passivity over the steel bars and retarded the onset of corrosion. It could reduce the total corroded area of steel bar for almost half of the tap water mixing.

(3) The results of 36-years exposure test of concrete mixed with seawater with concrete cover 50mm demonstrated high possibility of using seawater as a material of reinforced concrete, especially in marine tidal environment.

ACKNOWLEDGEMENT

Special gratitude is dedicated to Japan's Ministry of Education, Culture, Sports, Science, and Technology (MEXT) for providing financial study assistance to the first author.

REFERENCES

[1] JGC16, "Standard Specification for Concrete Structures (Materials and Construction)," Japan Society of Civil Engineers, 2007.

[2] Mohammed, T. U., T. Yamaji, A. Toshiyuki, and H. Hamada. "Marine durability of 15-year old concrete specimens made with ordinary Portland, slag and fly ash cement," ACI Spec., pp.199-30.

[3] Fukute, T., and H. Hamada. "A Study on the Durability of Concrete Exposed in Marine Environment for 20 Years." Report of the Port and Harbour Research Institute 31, no. 5, 1993.

[4] ASTM C 876-15, "Standard Test Method for Half-cell Potential of Uncoated Reinforcing Steel in Concrete," American Society for Testing and Materials, 2018.

[5] Otsuki, N. "A study of effectiveness of chloride on corrosion of steel bar in concrete." Report of Port and Harbor Research Institute, 1985, pp. 127-134.

[6] Ismail, Idawati, et al. "Influence of fly ash on the water and chloride permeability of alkali-activated slag mortars and concretes." Construction and Building Materials, 48, 2013, pp.1187-1201.

[7] Kayali, Obada, M. S. H. Khan, and M. Sharfuddin Ahmed. "The role of hydrotalcite in chloride binding and corrosion protection in concretes with ground granulated blast furnace slag." Cement and Concrete Composites, 34, No. 8, 2012, pp. 936-945.

[8] Adiwijaya. "Dissertation-A Fundamental Study on Seawater-Mixed Concrete Related to Strength, Carbonation and Alkali-Silica Reaction." Kyushu University, Sept 2015.

[9] Midgley, H. G., and J. M. Illston. "Effect of chloride penetration on the properties of hardened cement pastes." 7th international congress on the chemistry of cement, Vol. 3., 1986, pp. 101-103.